



HAL
open science

Quantification of right ventricular extracellular volume in pulmonary hypertension using cardiac magnetic resonance imaging

P. Habert, T. Capron, S. Hubert, Z. Bentatou, A. Bartoli, F. Tradi, S.
Renard, S. Rapacchi, Maxime Guye, Monique Bernard, et al.

► To cite this version:

P. Habert, T. Capron, S. Hubert, Z. Bentatou, A. Bartoli, et al.. Quantification of right ventricular extracellular volume in pulmonary hypertension using cardiac magnetic resonance imaging. *Diagnostic and Interventional Imaging*, 2020, 101 (5), pp.311-320. 10.1016/j.diii.2019.12.008 . hal-02457050

HAL Id: hal-02457050

<https://amu.hal.science/hal-02457050v1>

Submitted on 19 Nov 2020

HAL is a multi-disciplinary open access archive for the deposit and dissemination of scientific research documents, whether they are published or not. The documents may come from teaching and research institutions in France or abroad, or from public or private research centers.

L'archive ouverte pluridisciplinaire **HAL**, est destinée au dépôt et à la diffusion de documents scientifiques de niveau recherche, publiés ou non, émanant des établissements d'enseignement et de recherche français ou étrangers, des laboratoires publics ou privés.

Quantification of right ventricular extracellular volume in pulmonary hypertension assessed by cardiac magnetic resonance imaging: a feasibility study

Authors: Paul Habert^{1 2}, Thibaut Capron², Sandrine Hubert³, Zakaria Bentatou², Axel Bartoli¹, Farouk Tradi¹, Sebastien Renard³, Stanislas Rapacchi², Maxime Guye², Monique Bernard², Gilbert Habib³, Alexis Jacquier^{1 2}

Affiliations:

¹Service de radiologie et imagerie cardiovasculaire, Assistance Publique - Hôpitaux de Marseille, 13385, Marseille, France

²Aix-Marseille Université, UMR 7339, CNRS, CRMBM-CEMEREM (Centre de Résonance Magnétique Biologique et Médicale – Centre d’Exploration Métaboliques par Résonance Magnétique), Assistance Publique - Hôpitaux de Marseille, 13385, Marseille, France

³Service de cardiologie, Assistance Publique - Hôpitaux de Marseille, 13385, Marseille, France

Corresponding author (*mail and phone*): Dr. Paul Habert

paul.habert@ap-hm.fr ; +33413429081

Abstract count: environs 300 words (*150 - 250 words*) **Word count:** 2728 words (**4000 max**)

Keywords (*5 max*) : pulmonary hypertension ; 2D Strain ; cardiac magnetic resonance ; T1 mapping ; extracellular volume ; right ventricle fibrosis

Abstract

Purpose: The goal of that study was to assess the correlation of biventricular diffuse myocardial fibrosis in pulmonary hypertension (PH) as assessed by late gadolinium enhancement, extracellular volume (ECV) quantification with serum markers of collagen turnover and conventional prognostic markers from strain echocardiography.

Methods: Twelve patients with PH underwent the same day: Transthoracic echocardiography: including measurement of right ventricular (RV) fractional shortening (RVfs), tricuspid annular plane systolic excursion (TAPSE), maximal tricuspid annular velocity, RV global and segmental deformation. Right heart catheterization measuring pulmonary arterial pressures in mmHg and cardiac output in l/min. 1.5T cardiac MRI measuring: right ventricular volumes and ejection fraction, native, and 15min post contrast T1 mapping using modified look-locker inversion-recovery (MOLLI) sequence. Serum quantification of two biomarkers of collagen turnover and hematocrit.

Results: Global RV ECV, reflecting the quantity of myocardial fibrosis, was $34\% \pm 4.2$ for our entire population. A significant correlation was found between RV ECV and: RVfs ($r=0.6$, $p=0.026$) S'wave velocity ($r=0.7$, $p=0.009$), TAPSE ($r=0.6$, $p=0.040$) and RV systolic ejection fraction on the CMR ($r=0.6$, $p=0.04$). There was no correlation between the ECV values in the lateral wall of the RV and in the septum ($r=0.4$, $p=0.206$). A significant correlation between septal ECV and 2D septal strain ($r=0.7$, $p=0.013$) was found. Lastly, only a tendency was observed between the PIIINP values and RV ECV in a sub-group of 7 patients.

Conclusion: ECV quantification in PH appears to correlate with known echocardiographic prognostic markers and more specifically with the markers which assess RV systolic function. These results suggest that RV myocardial fibrosis measured with ECV could become a new prognostic parameter in PH.

INTRODUCTION

Pulmonary hypertension (PH) is a rare and severe condition defined by a rest mean pulmonary artery pressure (mPAP) exceeding 25 mmHg, measured by right heart catheterization (RHC) [1]. Prognosis is drastically affected by the ability of the right ventricle (RV) to adapt to chronic afterload increase [2]. Functional imaging evaluation of the right ventricle is thus essential to determine disease severity.

RHC is an invasive procedure and transthoracic echography (TTE) has become routinely used for screening of elevated pulmonary artery pressure. RV function is also assessed by TTE through different parameters: tricuspid annular plane systolic excursion (TAPSE), S wave velocity, eccentricity index and right ventricle outflow tract fractional shortening (RVfs). However, for anatomical and physiological reasons, echographic exploration of RV function remains difficult. In addition, most of the indices are prone to preload variability [3]. Over the past few years, TTE functional evaluation using 2D strain has shown promising results in RV follow-up for PH [4,5].

Cardiac magnetic resonance (CMR) has become the gold standard for non-invasive morphological and functional assessment of RV [6–8]. In addition, CMR can be used to assess myocardial fibrosis using contrast-enhancement sequences with gadolinium injection [9–11]. Myocardial replacement fibrosis is assessed by late gadolinium-induced enhancement (LGE) and myocardial interstitial fibrosis is reflected by the extra-cellular volume (ECV) fraction measured using native and post-contrast T_1 maps [12]. However this technique is difficult to use for the RV because of insufficient spatial resolution with respect to RV wall thickness. Only

few studies have previously addressed RV T₁-mapping, showing correlation between post-contrast T₁ and decreased RV ejection fraction (RVEF) or strain in non-ischemic cardiomyopathies, attributed to myocardial fibrosis influence [13,14].

In PH, LGE has been debated to show correlation with factors of adverse outcome [15]. Actually, LGE at ventricular insertion points is a typical feature of PH but was reported to rather reflect myocardial disarray than fibrosis [16]. Subsequently, T1-contrast has been evaluated at ventricular insertion points in PH; T1 value was found increased in PH patients [17] and associated with biventricular function [17,18]. In a chronic PH model, T1 and ECV at ventricular insertion points appeared to be early correlated to pulmonary hemodynamics [19].

In this study, we examined the feasibility of measuring global ECV fraction in RV of patients with PH, not limited to ventricular insertion points. For consistency, results were compared to serum biomarkers of pro-fibrotic activity in myocardium and echocardiographic parameters for RV function, in particular RV longitudinal strain which have previously shown good correlation with RV myocardial fibrosis [20].

METHODS

Subjects

The study was accepted by the local ethical committee and written informed consent was obtained from all subjects, according to the Helsinki declaration. Patients referred to our cardiology PH center between January 2012 and March 2013 were prospectively enrolled

during a single hospitalization. Inclusion criteria were: age > 18 years and pre-capillary PH as defined by the European Society of Cardiology: mPAP \geq 25 mmHg and a pulmonary capillary pressure < 15 mmHg in RHC. Patients could be enrolled at diagnosis or at follow-up for reassessment of specific therapy efficacy. Exclusion criteria were: PH secondary to a cardiac congenital malformation, post capillary PH, patients carrying an implantable device such as pacemaker or defibrillator, claustrophobia, neurostimulator, cochlear implant, glomerular filtration rate < 30 mL.min⁻¹.1.73m⁻². Patients with insufficient quality of CMR sequences were excluded.

Clinical and PH assessment data

Collection of clinical data included: age, gender, weight, height, etiology of PH as classified by Dana Point 2009 [21], treatment with loop diuretics (furosemide) or specific treatment for PH, NYHA stage of dyspnea, syncope or lipothymia signs, rest pulse oxygen saturation. A 6-minute-walk-distance (6MWD) test was performed under adequate oxygen support (results in meters and percentage of the theoretical value for age). Brain natriuretic peptide (BNP) was measured in blood sample. Pulmonary hemodynamic data was obtained from RHC performed following standard recommendations [22], yielding pulmonary artery pressures (systolic, diastolic and mean) and cardiac output (CO).

Blood biomarkers of fibrosis

Measurement of serum biomarkers of collagen metabolism, reflecting pro-fibrotic activity in the myocardium, was used to assess fibrosis. This method has already shown promising results in the evaluation of left ventricle myocardial fibrosis [23,24]. They were measured by enzyme

immunoassay (Siemens) on blood samples taken the same day as CMR, after a resting period of 20 minutes. Two markers were evaluated for collagen synthesis: PIII-NP (Procollagen III - N-Propeptid) and a biomarker for degradation of collagen: TIMP-1 (Tissue Inhibitor of Metalloproteinase-1).

Ultrasound data

TTE was performed on a commercial sonographer (Vivid 7 ultrasound General Electric Medical System) by a trained operator blinded to other results. The following parameters were recorded: systolic PAP (sPAP), right ventricular visual assessment, RVfs, S' wave, TAPSE, diastolic and systolic RV surfaces (SRV), left ventricular ejection fraction (LVEF) and presence or absence of pericardial effusion.

Myocardial deformation was measured by 2D strain using Speckle Tracking Imaging [25]. This technique consists in semi-automatic segmentation of endocardial and epicardial contours of the RV wall on a kinetic loop; myocardium contraction is regionally assessed following modification of the contour throughout the cardiac cycle. The main marker obtained is the RV global longitudinal strain as an objective index of RV systolic function with prognostic significance (Figure 1) [25]. The technique yields indexes of longitudinal septal and lateral strains, whose averaging gives the global strain.

CMR protocol

CMR protocols were performed on a 1.5 T whole-body MR scanner (Symphony TIM, Siemens, Erlangen, Germany) using a dedicated 12-element array coil with the patient placed in a supine

position. Images were acquired during a full inspiratory breath-hold with ECG gating.

Three types of sequences were used:

1) Ventricular function was assessed using steady state free precession (SSFP) short-axis cine slices acquired with the following parameters: TR/TE = 3.6ms/1.8ms, slice thickness = 7 mm, flip angle = 65°, spatial resolution = 1.3 x 1.3 mm², temporal resolution = 35 ms. A stack of short-axis slices was prescribed in order to cover RV from base to apex. These sequences allowed for kinetic analysis and calculation of RVEF following Simpson's rules [26].

2) T₁-mapping was obtained with modified look-locker inversion recovery (MOLLI) sequence with a single-shot balanced steady-state free precession (bSSFP) readout and parameters TR/TE = 2.4ms/1.2ms, flip angle = 35°, thickness = 7 mm, spatial resolution 2.3 x 2.3 mm², 3 inversions pulses with 4, 3 and 2 images acquired after each inversion pulse respectively and 1 heart beats to recover before the 2nd and the 3rd inversion [27]. MOLLI T₁-mapping was performed before and 15 min after intra-venous gadolinium injection (Dotarem®, 0.2 mmol/kg) followed by a 20 mL flash of saline solution. Three slices in short-axis view were placed at basal, middle and apex of RV.

3) Late gadolinium enhancement (LGE) was acquired 10 minutes after contrast injection in order to identify RV replacement fibrosis. This was obtained with a Gradient echo sequence: TR/TE = 650/1.56 ms, slice thickness = 6 mm, flip angle = 10°, spatial resolution 1.3 x 1.3 mm². The inversion time = 270-325 ms was manually set so as to cancel the T₁ signal of myocardium at the end-diastolic phase. 14 short-axis slices were prescribed to encompass the right ventricle in a single breath-hold.

Image post processing

RV volumes, ejection fraction and mass were determined on the SSFP images using semi-automated software (Argus, Siemens Healthcare, Erlangen, Germany) following standard method [28].

T_1 maps were reconstructed offline from MOLLI images as previously described, using the "MRMap" software available from <http://sourceforge.net/projects/mrmap/>. The images were sorted by their effective TI to perform a three parameter nonlinear curve fitting using a Levenberg-Marquardt algorithm of the following equation $y = A - B \exp(-t/T_1^*)$, yielding T_1^* , the longitudinal relaxation time under partial saturation. T_1 was then calculated from T_1^* as in conventional Look-Locker methods by $T_1 = T_1^* ((B / A) - 1)$ [29].

Native and post-contrast T_1 maps were further interpolated using Osirix (Lancros 5, Geneva, Switzerland) yielding final resolution of $0.5 \times 0.5 \text{ mm}^2$ for analysis. For each slice, RV was first divided in three segments on the lateral wall and one segment on the trabeculae septomarginalis (Figure 2). LV was also divided following standard method (6 segments at basal and middle levels, 4 at apex).

In PH patients, myocardium of the right ventricle was thickened due to chronic right heart afterload increase and this allowed for controlling partial volume artifact in RV regions of interest (ROI) delimitation. If thickness was larger than 5 mm, corresponding to ten times larger than effective resolution, a ROI was manually drawn in each segment of RV and LV myocardium, as described previously (Figure 3). Areas presenting with LGE positivity were excluded in the manual delimitation so as to exclude replacement fibrosis from ECV interstitial

fibrosis assessment. Most of the time the LGE was found close to the superior and inferior right ventricular insertion points. Rarely inferior RV wall was not thick enough (< 5 mm) to allow for reliable ECV quantification, in these cases this ROI has not been accounted for ECV. ECV was calculated in each ROI following well-established formula based on variation of longitudinal relaxation time T_1 15 minutes after contrast injection and using blood hematocrits of the patient [30,31].

Statistical analysis

Results were expressed as mean with standard deviation unless otherwise stated. Non-parametric Mann-Whitney tests were used for categorical variables according to the sample size (N=12). The relationship between quantitative parameters was examined with Spearman correlation test. Bilateral statistical tests < 0.05 were considered significant. Statistical analysis was performed on SPSS Version 20.0 software (IBM Inc., New York, USA).

RESULTS

Between January 2012 and March 2013, 21 patients presenting with PH in our center were enrolled. ECV calculation was not possible on the RV free wall for 9 patients due to either motion artifact or inability to hold repeated apnea. Subsequently 12 patients were included in the study. The mean age of the population was 50 ± 16 years, 6 males and 6 females, mean weight 63.5 ± 13.4 kg, mean height 166.5 ± 16.3 cm.

The etiology of PH was mainly idiopathic (41.7%) or secondary to connective tissue disease (33.3%). Clinically, our population was at an advanced stage of the disease, with a majority of patients presenting NYHA III dyspnea (7 patients - 58.3%) and altered 6MWD (group mean 57.4 % of theoretic for age). Characteristics of the patients are detailed in Table 1.

In the group considered, mean BNP was elevated to 272 ng/L, mean mPAP 44 mmHg and mean TTE LVEF was preserved at 61.3 %. Global RV strain was altered, either on RV septum and on RV free wall (global RV strain -18.3 ± 4.8 %); normal value is inferior than -20 % [32]. Global RV and LV ECV were elevated respectively 34.0 ± 4.2 % and 30.6 ± 3.8 %. Summary of hemodynamic, echographic and CMR data is presented in Table 2.

A significant correlation coefficient was found between RV ECV values and the following prognostic parameters for PH: RVfs, S' wave, TAPSE, RVEF_{MRI} (Figure 4). The strongest correlation was found for the S' wave with a Spearman coefficient of $r = -0.71$, ($p = 0.009$).

Concerning RV strain a significant correlation was found between septum RV ECV values and septal RV strain $r = 0.7$ ($p = 0.013$) (Figure 5).

Blood biomarkers of fibrosis were available in only 7 patients among the 12 due to a technical incident. RV ECV fraction was lower in the groups of negative TIMP-1 and negative PIII-NP (Figure 6) but results were not statistically significant in this subgroup ($p=0.105$ for TIMP-1 and $p=0.064$ for PIII-NP).

DISCUSSION

This study shows the feasibility to assess RV ECV fraction in PH patients with CMR. Results correlate with echographic markers of RV function and RV strain in septum. Blood markers for fibrosis also showed tendency to correlation with RV ECV though results did not reach statistical significance.

Myocardial fibrosis has been mainly studied and measured with CMR in the left ventricle. Histological correlation has been established based on LGE measurements and ECV assessment of diffuse interstitial fibrosis [33,34]. Our results on RV are consistent with a relation between RV ECV quantification and myocardial fibrosis.

Quantification of ECV in right ventricular wall is challenging because RV free wall is thin, leading to potential partial volume effects with epicardial RV fat. In PH patients with right chronic afterload, RV wall thickened significantly, allowing for selection of areas where the RV wall was ten times larger than effective image resolution. This is not the case in most other studies investigating RV ECV, selecting ROIs at ventricular insertion points. These regions were also avoided in our work using LGE, as their histologic nature is not clear in PH.

All the RV ECV values we recorded were > 25 % and thus higher than the normal value for LV [35]. To date, there is no data on normal RV ECV values in volunteers. In our work, LV ECV values were also collected in order to allow for comparison. Global RV ECV was larger than LV ECV on segments other than septum, supporting the right-sided specific impact from chronic afterload increase in pre-capillary PH.

In several patients the RV wall was so thin that the measurements could not be assessed, due to motion artifacts. This could be improved by the use of navigator-gated accelerated sequences reducing motion artifacts and giving better definition of RV [36].

A significant correlation was found between the RV ECV values and echocardiographic and MRI surrogate markers of prognostic in PH: TAPSE, S' wave velocity, RVfs and RVEF_{MRI}. No correlation was found with NYHA class or 6MWD. The value of RV ECV as a surrogate marker of prognosis in PH might be interesting to assess in a larger study. Another study from Mehta *et al.* found similar results with a significant linear correlation between RV ECV and RVEF, RV end diastolic volume using CMR accelerated navigator-gated sequences [37]. In the same study the RV ECV was greater than LV ECV in PH and RV ECV was nearly equivalent to LV ECV in normal volunteers, showing again an increase in ventricular fibrosis predominating on RV.

The RV ECV calculated on the interventricular septum and septal RV longitudinal strain were correlated. 2D Strain echography has already demonstrated its prognostic value in PH for assessing RV systolic function and monitoring the efficiency of treatment with vasodilators [38,39]. Interstitial fibrosis could lead to a reduction of cardiac motion. This result reinforces the hypothesis that ECV could be a marker which should enable us to refine the parameters of RV systolic function and may represent a new prognostic marker to guide treatment and follow-up.

Regarding blood biomarkers of fibrosis, there was a trend towards significance for the correlation between TIMP-1, PIIINP and RV ECV in a sub-group of 7 patients. PIII-NP was first studied in ischemic heart disease and its over-expression seemed to be related to the

formation of a fibrotic scar as a result of myocardial infarction [40]. Following this, Sipola *et al.* demonstrated that high levels of PIII-NP were significantly linked to the presence of LGE on CMR in a genetically predetermined population of patients with hypertrophic cardiomyopathy [41]. In RV disorders, there is only one study showing a correlation between the collagen synthesis biomarkers (PIII-NP and TIMP-1) and RV dysfunction in patients operated for tetralogy of Fallot [42].

The main limitation of this work was the low number of patients. First, inclusion of patients with a pre-capillary PH is an infrequent condition compared to post-capillary PH [43]. Second, dyspneic patients with PH have difficulties to perform an apnea-based examination. Even with a selection of patients likely to perform the examination, some patients were unable to maintain apnea or supine position throughout the duration of the examination during an hour. Among the 21 patients initially screened, only 12 had sufficient quality image allowing for interpretation.

Another limitation of this work is the inhomogeneity of the population studied regarding stage of the disease; all patients referred were considered, from initial diagnosis to follow-up after several years under specific treatment.

In conclusion, quantification of ECV using T_1 mapping in a population of patients with PH seems to be a feasible technique for assessing RV interstitial myocardial fibrosis. Apnea-based CMR examination currently limits wide use in such dyspneic population but navigator-gated accelerated protocols may overcome this limitation. RV interstitial fibrosis assessment should be further confirmed on a larger population and may be correlated with direct histologic fibrosis. Clinical significance of this RV fibrosis in PH could also be investigated more accurately in future works.

ACKNOWLEDGEMENTS:

This work was supported by Aix-Marseille Université and CNRS (UMR 7339). This work was performed by a laboratory member of France Life Imaging network (grant ANR-11-INBS-0006).

Tables

Table 1 : Characteristics of patients

		<i>Total Population</i>
<i>Number of patients</i>		12
<i>Demographic data</i>		
Gender	Male	6 (50 %)
	Female	6 (50 %)
Weight (kg)		63.5 ± 13.4
Height (cm)		166.5 ± 16.3
Age (years)		50 ± 16
Etiology of PH	Idiopathic	5 (41.7%)
	Connectivitis	4 (33.3%)
	Post embolic	2 (16.7%)
	Cirrhosis	1 (8.3%)
<i>Clinical data</i>		
NYHA scale	1	0 (0%)
	2	4 (33.3%)
	3	7 (58.3%)
	4	1 (8.3%)
Lipothymia-fainting		4 (33.3%)
Pulse oximetry at rest (%)		96 ± 2
6 min walk test (m)		349.3 ± 80.7
6 min walk test theoretical ratio (%)		57.4 ± 12.6

Table 1. Characteristics of the population and clinical data. The qualitative variables are expressed as figure with percentage and the continuous variables as mean values ± DS. PH : pulmonary hypertension.

Table 2 : Invasive / non invasive data**Total
Population**

Biological data		
BNP (ng/l)		271.8 ± 309.7
Hemodynamic data		
sPAP (mmHg)		68.1 ± 13.1
dPAP (mmHg)		29.2 ± 11.1
mPAP (mmHg)		43.9 ± 11.5
CO (L/min)		4.7 ± 1.4
Echographic data		
PAPs (mmHg)		65.3 ± 18.9
SRV diastole (cm ²)		28.3 ± 8.4
SRV systole (cm ²)		17.6 ± 6.5
LVEF (%)		61.3 ± 6.4
RVfs (%)		41.2 ± 8.9
S' wave velocity (cm/sec)		12.6 ± 3.5
TAPSE (mm)		21.6 ± 4.6
Visual RVEF	Intact	7 (58.3%)
	Moderately impaired	3 (25%)
	Severely impaired	2 (16.7%)
Pericardial effusion		6 (50%)
Global Strain (%)		-18.3 ± 4.8
Lateral Strain (%)		-15.5 ± 11.6
Septal Strain (%)		-19.8 ± 3.2
Cardiac MRI data		
RVEF _{MRI} (%)		40 ± 18
Indexed RV EDV (ml/m ²)		97.1 ± 22.2
Indexed RV ESV (ml/m ²)		61.6 ± 22.2
Indexed mass (g/m ²)		31.1 ± 6.6
CO (L/m ²)		4.7 ± 1.5
Global RV ECV (%)		34.0 ± 4.2
Lateral RV ECV (%)		33.7 ± 6.2
Septal RV ECV (%)		34.2 ± 4.2
Lateral wall and trabecula septomarginalis RV ECV (%)		33.8 ± 6.2
Septal LV ECV (%)		33.9 ± 4.3
Anterior, lower and lateral wall LV ECV (%)		30.6 ± 3.8

Table 2. Biological, echocardiographic and CMR data. The qualitative variables are expressed as figures with percentage and the continuous variables as mean values ± DS. BNP : Brain natriuretic peptide, CO : cardiac output, dPAP : diastolic pulmonary arterial pressure, ECV : extracellular volume, EDV : end diastolic volume, ESV : end systolic volume, LV : left ventricular, LVEF : left ventricular ejection fraction, mPAP : mean pulmonary arterial pressure, PAPs : pulmonary arterial pressure obtained by echocardiography, RV : right ventricle, RVEF :

right ventricular ejection fraction RVfs : right ventricular fraction shortening, sPAP : systolic pulmonary arterial pressure, SRV : surface of right ventricle, TAPSE : tricuspid annular plane systolic excursion.

FIGURES

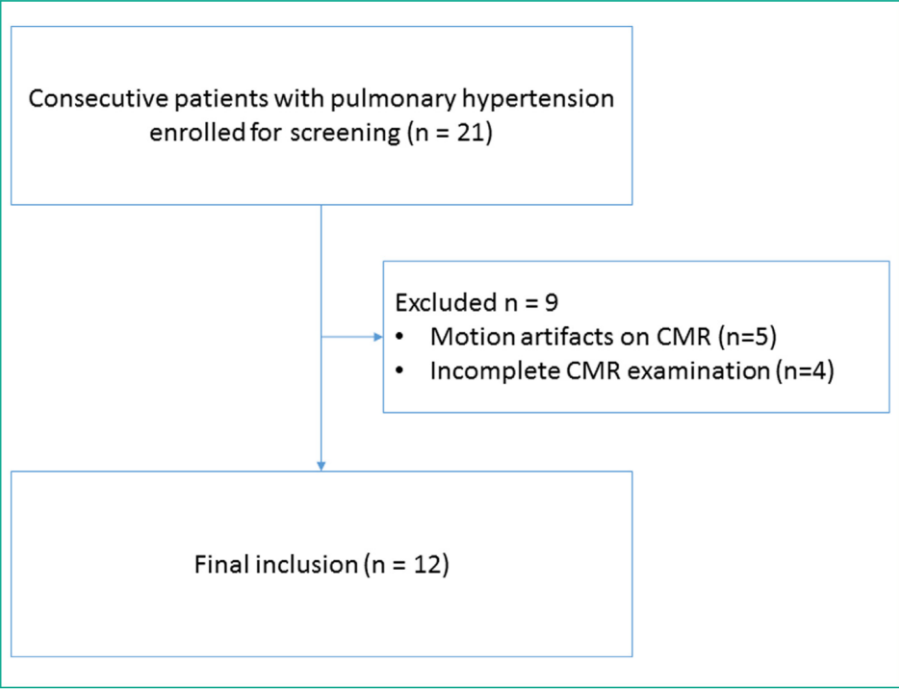


Figure 1. Flowchart shows patient selection process based on inclusion and exclusion criteria.

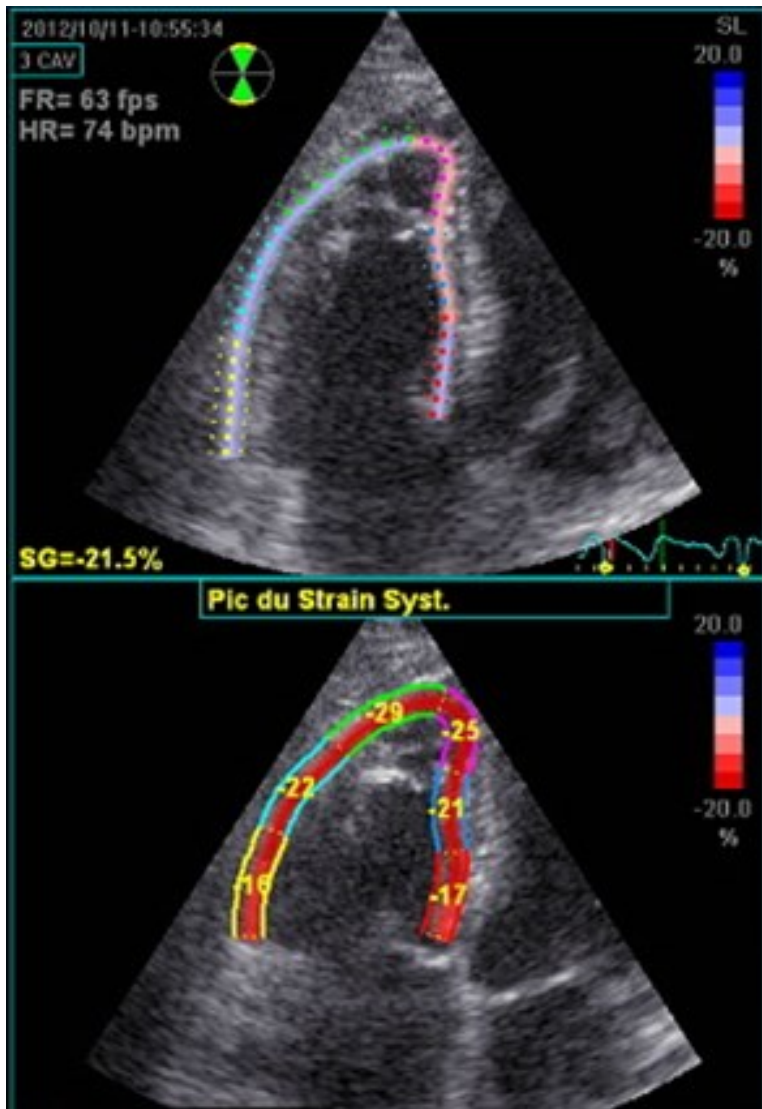


Figure 2: 2D sonography using dedicated software to analysis global and segmental strain of the right ventricle, after manual segmentation.

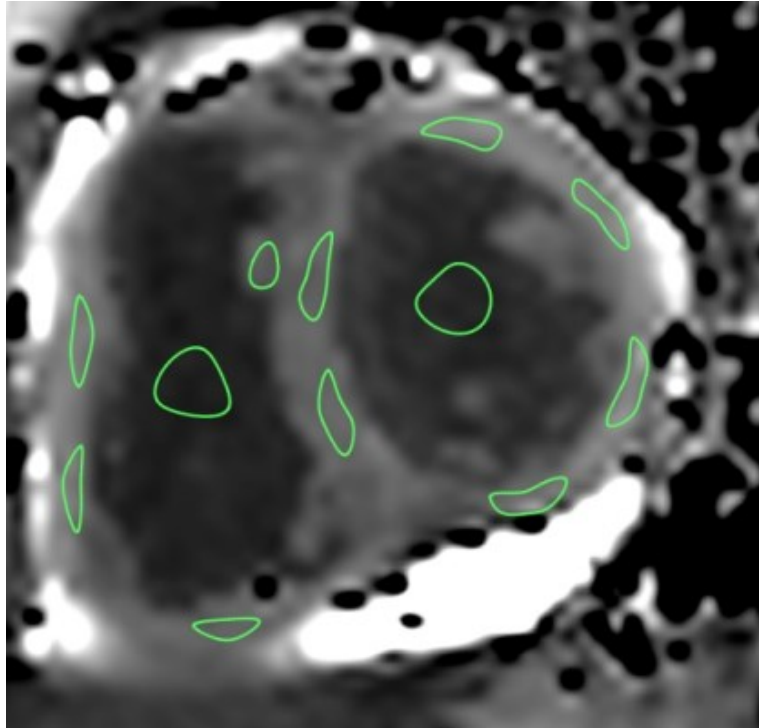


Figure 3: MOLLI sequence in short axis at mid ventricular for ECV quantification. Length of myocardial wall 9 minutes post gadolinium enhancement. The RV has been segmented into four: 2 of the sidewall 1 inferior and 1 on the moderator band. That corresponds to 12 segments for the RV (4 at the apex, 4 and 4 middle portion at the base). The LV has been divided into six: 1 in front, 2 of the septal wall, 1 inferior, 2 on the sidewall. 18 segments for LV (6 apex, 6 mid and 6 base).

This figure shows the way to draw ROI in the myocardium, they are deliberately wide in order to avoid partial volume artifacts.

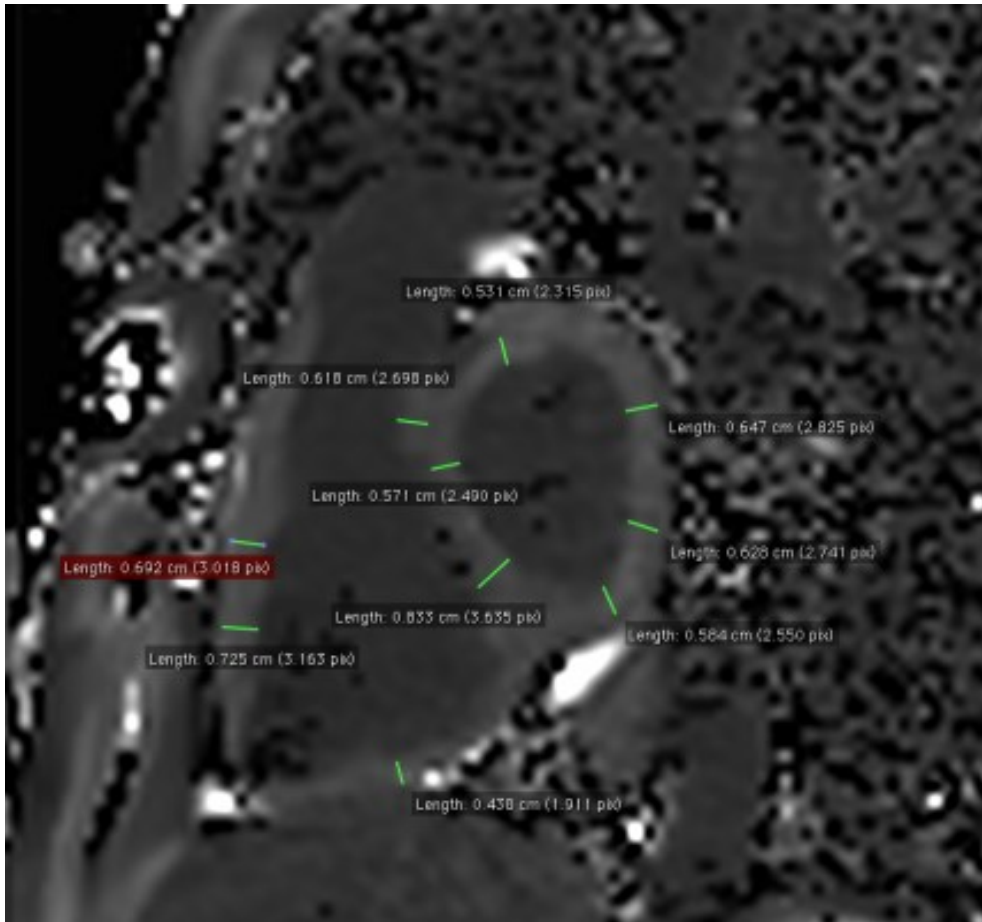


Figure 4: MOLLI sequence 9 minutes post gadolinium enhancement in short axis at mid ventricular, allowing ECV quantification. Lengths of myocardial wall are measured, in order to view walls' portion upper than 5 mm which could be analyzed. Some ROI have not been placed on pre-defined segments due to a RV wall thickness less than 5 mm.

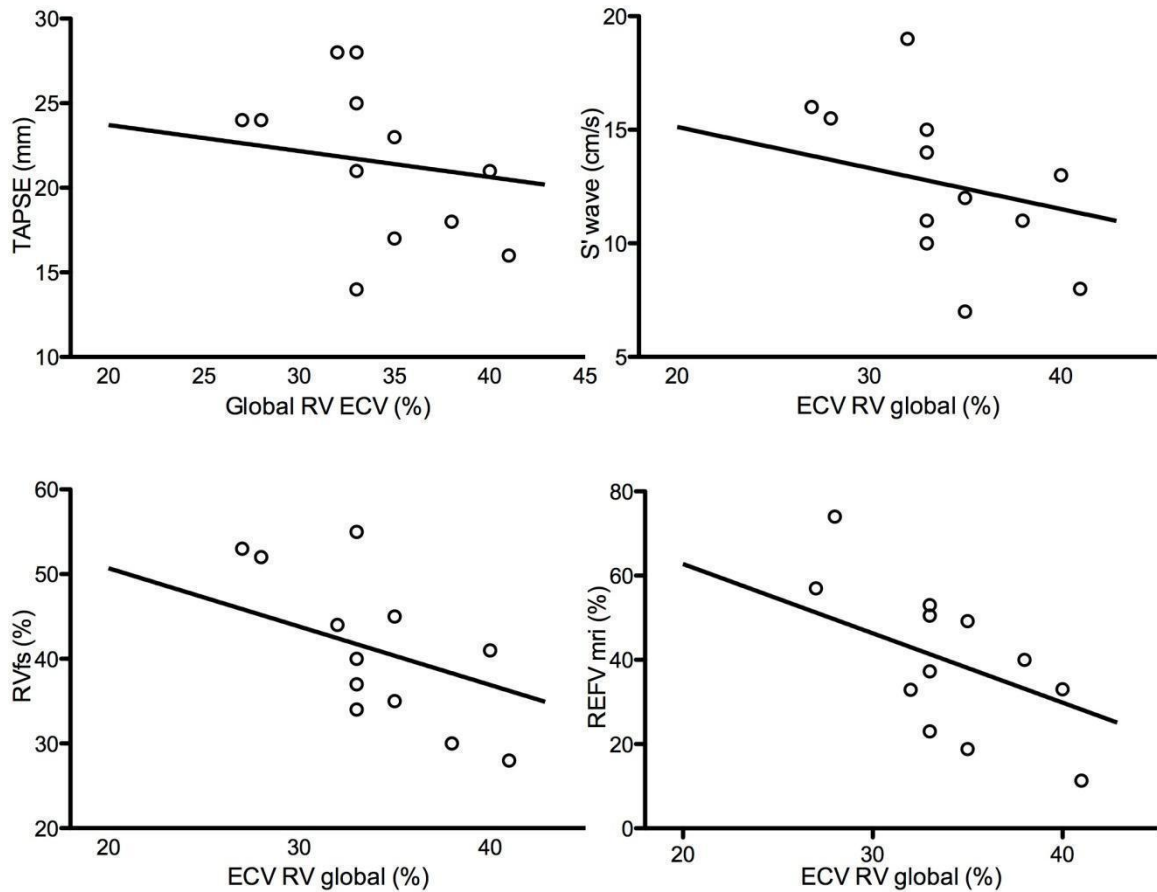


Figure 5a: Linear regression showing significant correlation between global RV ECV (%) and TAPSE (mm) ; S' wave (cm/s) ; RVsf (%) ; RVEF_{MRI} (%). Spearman correlation are: $r = -0.59$ $p = 0.04$; $r = -0.71$ $p = 0.009$; $r = -0.64$ $p = 0.026$; $r = -0.59$, $p = 0.04$ respectively.

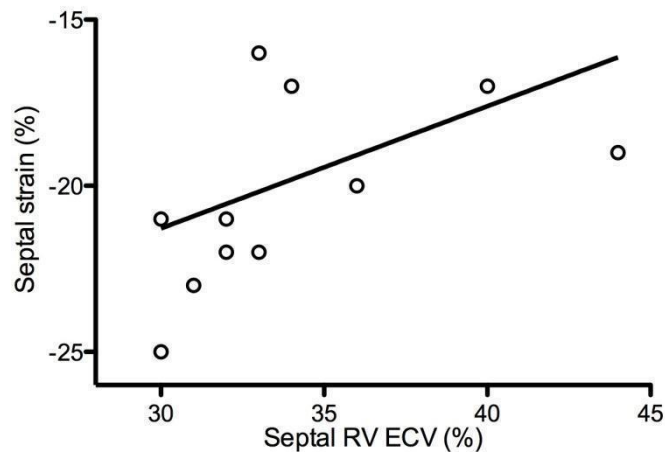


Figure 5b: Linear regression showing significant correlation between septal RV ECV (%) and average septal Strain (%) with a Spearman coefficient $r = 0.69$; $p = 0.013$. The higher the interstitial fibrosis in the septum, the lower the myocardial contractility of the septum.

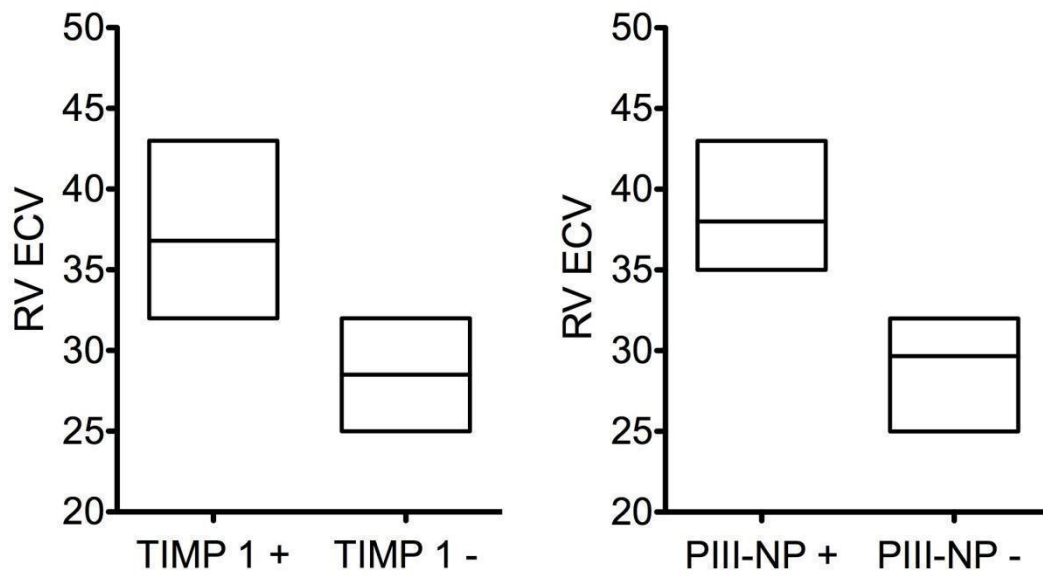


Figure 6: Diagram showing the trend of distribution of ECV between patients with a positive biological assay for TIMP-1 or TIII-NP. Analysis in a subgroup of 7 patients. There is a clear trend towards a higher percentage of ECV in patients with a positive biological assay ($p = 0.105$ for TIMP1 and $p = 0.064$ for PIII-NP).

Reference list

1. “2015 ESC/ERS Guidelines for the diagnosis and treatment of pulmonary hypertension. The Joint Task Force for the Diagnosis and Treatment of Pulmonary Hypertension of the European Society of Cardiology (ESC) and the European Respiratory Society (ERS).” Nazzareno Galiè, Marc Humbert, Jean-Luc Vachiery, Simon Gibbs, Irene Lang, Adam Torbicki, Gérald Simonneau, Andrew Peacock, Anton Vonk Noordegraaf, Maurice Beghetti, Ardeschir Ghofrani, Miguel Angel Gomez Sanchez, Georg Hansmann, Walter Klepetko, Patrizio Lancellotti, Marco Matucci, Theresa McDonagh, Luc A. Pierard, Pedro T. Trindade, Maurizio Zompatori and Marius Hoeper. *Eur Respir J* 2015; 46: 903-975. *Eur Respir J.* 2015;46: 1855–1856.
2. Handa S, Akaishi M, Iwanaga S, Yoshikawa T, Abe S, Yamada T, et al. [Prognosis of patients with primary pulmonary hypertension]. *J Cardiol.* 1989;19: 877–884.
3. Dutta T, Aronow WS. Echocardiographic evaluation of the right ventricle: Clinical implications. *Clin Cardiol.* 2017;40: 542–548.
4. Vitarelli A, Mangieri E, Terzano C, Gaudio C, Salsano F, Rosato E, et al. Three-dimensional echocardiography and 2D-3D speckle-tracking imaging in chronic pulmonary hypertension: diagnostic accuracy in detecting hemodynamic signs of right ventricular (RV) failure. *J Am Heart Assoc.* 2015;4: e001584.
5. Wright LM, Dwyer N, Celermajer D, Kritharides L, Marwick TH. Follow-Up of Pulmonary Hypertension With Echocardiography. *JACC Cardiovasc Imaging.* 2016;9: 733–746.
6. Kondo C, Caputo GR, Semelka R, Foster E, Shimakawa A, Higgins CB. Right and left ventricular stroke volume measurements with velocity-encoded cine MR imaging: in vitro and in vivo validation. *AJR Am J Roentgenol.* 1991;157: 9–16.
7. Sechtem U, Pflugfelder PW, Gould RG, Cassidy MM, Higgins CB. Measurement of right and left ventricular volumes in healthy individuals with cine MR imaging. *Radiology.* 1987;163: 697–702.
8. Rominger MB, Bachmann GF, Pabst W, Rau WS. Right ventricular volumes and ejection fraction with fast cine MR imaging in breath-hold technique: applicability, normal values from 52 volunteers, and evaluation of 325 adult cardiac patients. *J Magn Reson Imaging.* 1999;10: 908–918.
9. Wu KC, Weiss RG, Thiemann DR, Kitagawa K, Schmidt A, Dalal D, et al. Late gadolinium enhancement by cardiovascular magnetic resonance heralds an adverse prognosis in nonischemic cardiomyopathy. *J Am Coll Cardiol.* 2008;51: 2414–2421.
10. Leyva F, Taylor RJ, Foley PWX, Umar F, Mulligan LJ, Patel K, et al. Left ventricular midwall fibrosis as a predictor of mortality and morbidity after cardiac resynchronization therapy in patients with nonischemic cardiomyopathy. *J Am Coll Cardiol.* 2012;60: 1659–1667.
11. Moon JCC, McKenna WJ, McCrohon JA, Elliott PM, Smith GC, Pennell DJ. Toward clinical risk assessment in hypertrophic cardiomyopathy with gadolinium cardiovascular magnetic resonance. *J Am Coll Cardiol.* 2003;41: 1561–1567.

12. Messroghli DR, Moon JC, Ferreira VM, Grosse-Wortmann L, He T, Kellman P, et al. Clinical recommendations for cardiovascular magnetic resonance mapping of T1, T2, T2* and extracellular volume: A consensus statement by the Society for Cardiovascular Magnetic Resonance (SCMR) endorsed by the European Association for Cardiovascular Imaging (EACVI). *J Cardiovasc Magn Reson*. 2017;19: 75.
13. Jellis CL, Yingchoncharoen T, Gai N, Kusunose K, Popović ZB, Flamm S, et al. Correlation between right ventricular T1 mapping and right ventricular dysfunction in non-ischemic cardiomyopathy. *Int J Cardiovasc Imaging*. 2017; doi:10.1007/s10554-017-1113-3
14. Jellis C, Yingchoncharoen T, Ayache A, Flamm S, Kwon D. Right ventricular T1 mapping is technically feasible and correlates with right ventricular dysfunction in non-ischemic cardiomyopathy. *J Cardiovasc Magn Reson*. 2014;16: P336.
15. Freed BH, Gomberg-Maitland M, Chandra S, Mor-Avi V, Rich S, Archer SL, et al. Late gadolinium enhancement cardiovascular magnetic resonance predicts clinical worsening in patients with pulmonary hypertension. *J Cardiovasc Magn Reson*. 2012;14: 11.
16. De Lazzari M, Cipriani A, Rizzo S, Famoso G, Giorgi B, Tarantini G, et al. Right Ventricular Junctional Late Gadolinium Enhancement Correlates With Outcomes in Pulmonary Hypertension. *JACC Cardiovasc Imaging*. 2019; doi:10.1016/j.jcmg.2018.11.019
17. Reiter U, Reiter G, Kovacs G, Adelsmayr G, Greiser A, Olschewski H, et al. Native myocardial T1 mapping in pulmonary hypertension: correlations with cardiac function and hemodynamics. *Eur Radiol*. 2017;27: 157–166.
18. Chen YY, Yun H, Jin H, Kong DH, Long YL, Fu CX, et al. Association of native T1 times with biventricular function and hemodynamics in precapillary pulmonary hypertension. *Int J Cardiovasc Imaging*. 2017; doi:10.1007/s10554-017-1095-1
19. García-Álvarez A, García-Lunar I, Pereda D, Fernández-Jimenez R, Sánchez-González J, Mirelis JG, et al. Association of myocardial T1-mapping CMR with hemodynamics and RV performance in pulmonary hypertension. *JACC Cardiovasc Imaging*. 2015;8: 76–82.
20. Lisi M, Cameli M, Righini FM, Malandrino A, Tacchini D, Focardi M, et al. RV Longitudinal Deformation Correlates With Myocardial Fibrosis in Patients With End-Stage Heart Failure. *JACC Cardiovasc Imaging*. 2015;8: 514–522.
21. Humbert M, McLaughlin VV. The 4th World Symposium on Pulmonary Hypertension. *J Am Coll Cardiol*. 2009;54: S1–S2.
22. Hoeper MM, Bogaard HJ, Condliffe R, Frantz R, Khanna D, Kurzyna M, et al. Definitions and diagnosis of pulmonary hypertension. *J Am Coll Cardiol*. 2013;62: D42–50.
23. Takawale A, Zhang P, Patel VB, Wang X, Oudit G, Kassiri Z. Tissue Inhibitor of Matrix Metalloproteinase-1 Promotes Myocardial Fibrosis by Mediating CD63-Integrin β 1 Interaction. *Hypertension*. 2017; doi:10.1161/HYPERTENSIONAHA.117.09045
24. Ferreira JM, Ferreira SM, Ferreira MJ, Falcão-Pires I. Circulating Biomarkers of Collagen Metabolism and Prognosis of Heart Failure with Reduced or Mid-Range Ejection Fraction. *Curr*

Pharm Des. 2017; doi:10.2174/1381612823666170317124125

25. Lee J-H, Park J-H. Strain Analysis of the Right Ventricle Using Two-dimensional Echocardiography. *JACC Cardiovasc Imaging*. 2018;26: 111–124.
26. Schiller NB, Shah PM, Crawford M, DeMaria A, Devereux R, Feigenbaum H, et al. Recommendations for quantitation of the left ventricle by two-dimensional echocardiography. American Society of Echocardiography Committee on Standards, Subcommittee on Quantitation of Two-Dimensional Echocardiograms. *J Am Soc Echocardiogr*. 1989;2: 358–367.
27. Messroghli DR, Radjenovic A, Kozerke S, Higgins DM, Sivananthan MU, Ridgway JP. Modified Look-Locker inversion recovery (MOLLI) for high-resolution T1 mapping of the heart. *Magn Reson Med*. 2004;52: 141–146.
28. Jacquier A, Thuny F, Jop B, Giorgi R, Cohen F, Gaubert J-Y, et al. Measurement of trabeculated left ventricular mass using cardiac magnetic resonance imaging in the diagnosis of left ventricular non-compaction. *Eur Heart J*. 2010;31: 1098–1104.
29. Taylor AJ, Salerno M, Dharmakumar R, Jerosch-Herold M. T1 Mapping: Basic Techniques and Clinical Applications. *JACC Cardiovasc Imaging*. 2016;9: 67–81.
30. Arheden H, Saeed M, Higgins CB, Gao DW, Bremerich J, Wyttenbach R, et al. Measurement of the distribution volume of gadopentetate dimeglumine at echo-planar MR imaging to quantify myocardial infarction: comparison with ^{99m}Tc-DTPA autoradiography in rats. *Radiology*. 1999;211: 698–708.
31. Flett AS, Hayward MP, Ashworth MT, Hansen MS, Taylor AM, Elliott PM, et al. Equilibrium contrast cardiovascular magnetic resonance for the measurement of diffuse myocardial fibrosis: preliminary validation in humans. *Circulation*. 2010;122: 138–144.
32. Park J-H, Choi J-O, Park SW, Cho G-Y, Oh JK, Lee J-H, et al. Normal references of right ventricular strain values by two-dimensional strain echocardiography according to the age and gender. *Int J Cardiovasc Imaging*. 2018;34: 177–183.
33. Iles LM, Ellims AH, Llewellyn H, Hare JL, Kaye DM, McLean CA, et al. Histological validation of cardiac magnetic resonance analysis of regional and diffuse interstitial myocardial fibrosis. *Eur Heart J Cardiovasc Imaging*. 2015;16: 14–22.
34. Ravenstein C de M de, de Ravenstein C de M, Bouzin C, Lazam S, Boulif J, Amzulescu M, et al. Histological Validation of measurement of diffuse interstitial myocardial fibrosis by myocardial extravascular volume fraction from Modified Look-Locker imaging (MOLLI) T1 mapping at 3 T [Internet]. *Journal of Cardiovascular Magnetic Resonance*. 2015. doi:10.1186/s12968-015-0150-0
35. de Meester de Ravenstein C, de Ravenstein C de M, Bouzin C, Lazam S, Boulif J, Amzulescu M, et al. Histological Validation of measurement of diffuse interstitial myocardial fibrosis by myocardial extravascular volume fraction from Modified Look-Locker imaging (MOLLI) T1 mapping at 3 T. *J Cardiovasc Magn Reson*. 2015;17. doi:10.1186/s12968-015-0150-0
36. Mehta BB, Chen X, Salerno M, Kramer CM, Epstein FH. Accelerated and navigator-gated look-

- locker imaging for cardiac T1 Estimation (ANGIE) with reduced motion artifact. *J Cardiovasc Magn Reson.* 2012;14: O110.
37. Mehta BB, Auger DA, Gonzalez JA, Workman V, Chen X, Chow K, et al. Detection of elevated right ventricular extracellular volume in pulmonary hypertension using Accelerated and Navigator-Gated Look-Locker Imaging for Cardiac T1 Estimation (ANGIE) cardiovascular magnetic resonance. *J Cardiovasc Magn Reson.* 2015;17: 110.
 38. Motoji Y, Tanaka H, Fukuda Y, Ryo K, Emoto N, Kawai H, et al. Efficacy of right ventricular free-wall longitudinal speckle-tracking strain for predicting long-term outcome in patients with pulmonary hypertension. *Circ J.* 2013;77: 756–763.
 39. Haeck MLA, Scherptong RWC, Marsan NA, Holman ER, Schalij MJ, Bax JJ, et al. Prognostic value of right ventricular longitudinal peak systolic strain in patients with pulmonary hypertension. *Circ Cardiovasc Imaging.* 2012;5: 628–636.
 40. Ciccoira M, Rossi A, Bonapace S, Zanolla L, Golia G, Franceschini L, et al. Independent and additional prognostic value of aminoterminal propeptide of type III procollagen circulating levels in patients with chronic heart failure. *J Card Fail.* 2004;10: 403–411.
 41. Sipola P, Peuhkurinen K, Lauerma K, Husso M, Jääskeläinen P, Laakso M, et al. Myocardial late gadolinium enhancement is associated with raised serum amino-terminal propeptide of type III collagen concentrations in patients with hypertrophic cardiomyopathy attributable to the Asp175Asn mutation in the alpha tropomyosin gene: magnetic resonance imaging study. *Heart.* 2006;92: 1321–1322.
 42. Chen C-A, Tseng W-YI, Wang J-K, Chen S-Y, Ni Y-H, Huang K-C, et al. Circulating biomarkers of collagen type I metabolism mark the right ventricular fibrosis and adverse markers of clinical outcome in adults with repaired tetralogy of Fallot. *Int J Cardiol.* 2013;167: 2963–2968.
 43. Mocumbi AO, Thienemann F, Sliwa K. A global perspective on the epidemiology of pulmonary hypertension. *Can J Cardiol.* 2015;31: 375–381.